

## CHARM PHYSICS AT CDF II

Ivan K. Furić

(for the CDF II collaboration)

*M.I.T., Fermilab - CDF - MS#318, Batavia, IL 60510-0500*

### Abstract

The CDF II detector has the capability of triggering on displaced tracks. Because of this ability, CDF II has accrued large samples of charmed meson decays to fully hadronic final states in  $64 \text{ pb}^{-1}$  of  $p\bar{p}$  collision data gathered at  $\sqrt{s} = 1.96 \text{ TeV}$ . Using initial Run II data samples, the production cross sections for  $J/\psi$ ,  $D^0$ ,  $D^+$ ,  $D^{*+}$  and  $D_s^+$  mesons have been measured. Ratios of branching ratios for Cabibbo suppressed final states and  $CP$  asymmetries in  $D^0$  meson decays have been studied. A measurement of the mass difference  $m(D_s^+) - m(D^+)$  has been done, and a limit for the branching fraction of the FCNC  $D^0 \rightarrow \mu^+ \mu^-$  decays has been set.

## 1 Introduction

The CDF II detector <sup>1)</sup> is a major upgrade of the original CDF detector which last took data in 1996. In Run I of the Tevatron, CDF made important contributions to  $B$  physics, providing some of the best measurements of masses, lifetimes, mixing and branching ratios.

For charm physics results, the most important part of the upgrade are the new integrated tracking system and the new trigger system. The integrated tracking system consists of three silicon systems (L00 <sup>2)</sup>, SVXII <sup>3)</sup>, ISL <sup>4)</sup>) and a low-material, large-radius drift chamber (COT) <sup>5)</sup>. The detector has a brand new three-level trigger system. The new features of the trigger include triggering on muons with lower transverse momenta, and triggering on displaced tracks and vertices <sup>6)</sup>.

## 2 $J/\psi$ Production Cross Section

The mechanisms of  $J/\psi$  production in  $p\bar{p}$  collisions are not well understood. Production cross sections from the assumed two major sources,  $b \rightarrow J/\psi X$  and direct prompt decays, were measured to be higher than the initial theoretical predictions <sup>7)</sup>. Recent theoretical advances in the extraction of the non-perturbative fragmentation functions of the  $B$  mesons from LEP data in a way that is consistent with the NLO QCD calculations of the  $b$  hadroproduction cross-sections have improved agreement between theoretical predictions and CDF Run I  $b \rightarrow J/\psi X$  cross section measurements to better than 50 %.

The CDF II detector has an improved dimuon trigger with a lower  $p_T$  threshold ( $p_T > 1.4$  GeV/c). This has extended the low transverse momentum range of triggered  $J/\psi \rightarrow \mu^+ \mu^-$  down to  $p_T(\mu^+ \mu^-) \geq 0$  GeV/c. In 39.7 pb of the initial Run-II data, 300 000  $J/\psi \rightarrow \mu^+ \mu^-$  decays have been reconstructed. As shown in Figure 1, the transverse momentum of the reconstructed  $J/\psi$  extends to 0 GeV/c. After correcting for acceptance, trigger and reconstruction efficiencies, an integrated production cross section of  $240 \pm 1(stat)_{-28}^{+35}(syst)$  nb has been measured for  $J/\psi$  mesons with  $p_T(J/\psi) > 0$  GeV/c and  $|\eta(J/\psi)| < 0.6$ .

## 3 $D_s^+ - D^+$ Mass Difference

One of the first measurements done with the new sample of charmed meson decays was the measurement of the mass difference  $m(D_s^+) - m(D^+)$ . In a sample corresponding to  $11.6$  pb<sup>-1</sup>, 2 400  $D_s \rightarrow \phi\pi$  and 1 400  $D^+$  decays were reconstructed. The detector invariant mass resolution for these decays is about 8 MeV/c<sup>2</sup>. The momentum scale of the detector was calibrated using 50 000  $J/\psi \rightarrow \mu^+ \mu^-$  decays. An outline of the procedure is depicted in Figure 2. The

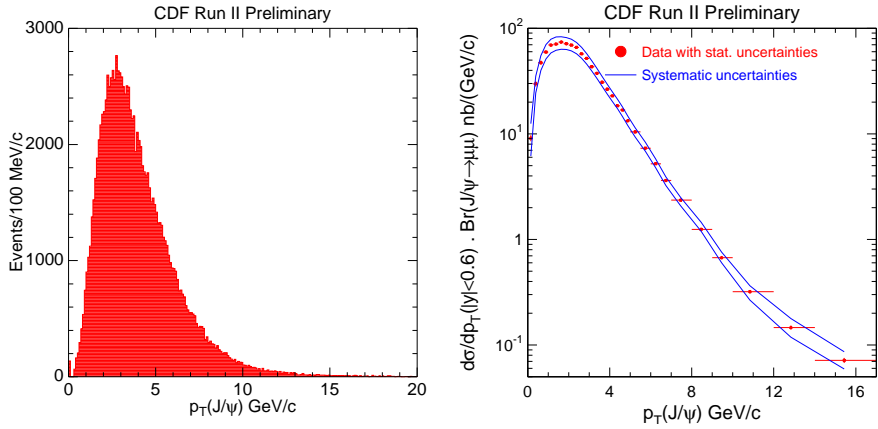


Figure 1:  $J/\psi$  cross section measurement: the left plot shows the  $p_T$  distribution of the reconstructed  $J/\psi$  mesons, and the right shows the differential production cross section ( $d\sigma/dp_T$ ).

invariant mass of the  $J/\psi$  decays shows a dependence on the transverse momentum of the reconstructed  $J/\psi$  because the energy loss in the tracking system is not accounted for. After accounting for energy loss according to the GEANT material map, a residual  $p_T$  dependence can still be seen. Conversion scans of the tracking volume confirm that there is material missing in the GEANT description so material is added by hand to remove the  $p_T$  dependence of the  $J/\psi$  mass. The magnetic field is scaled so that the  $J/\psi$  mass agrees with the world average <sup>8)</sup>. The results of the calibration (the amount of missing material and the magnetic field) are cross-checked by reconstructing other charmed and bottom meson decays ( $D^+, D^0, \Upsilon$ ), and the reconstructed masses are in good agreement with the corresponding world averages. This calibration was then applied to the  $D_s^+, D^+ \rightarrow \phi\pi$  decays and the mass difference was found to be  $m(D_s^+) - m(D^+) = 99.41 \pm 0.38(\text{stat}) \pm 0.21(\text{syst}) \text{ MeV}/c^2$ . The result is in good agreement with previous measurements <sup>9), 10)</sup>. The systematic error is dominated by signal and background modeling.

#### 4 Charmed Meson Production Cross Sections

In Run I, the B cross section for the  $B^+ \rightarrow J/\psi K^+$  mode for transverse momentum  $p_T(B^+) > 6 \text{ GeV}/c$  and rapidity  $|y(B^+)| < 1$  was measured to be

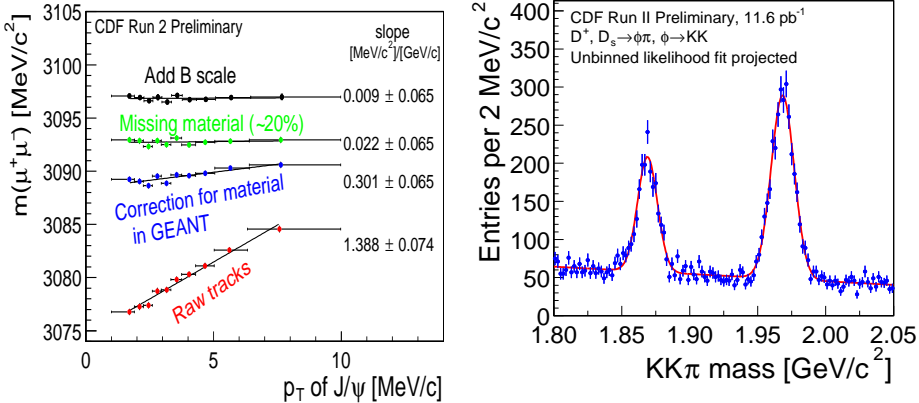


Figure 2: Momentum scale calibration and  $m(D_s^+) - m(D^+)$  mass measurement. The left plot depicts the momentum scale calibration procedure, and the right shows the invariant mass distribution for the  $D_s^+, D^+ \rightarrow \phi\pi$  signals with a superimposed fit.

$3.6 \pm 0.6 \mu\text{b}$  <sup>11)</sup>. A preliminary measurement of the cross section for  $D^0$ ,  $D^+$ ,  $D^{*+}$  and  $D_s^+$  mesons was done with  $5.7 \text{ pb}^{-1}$  of Run II data. The production cross sections were found to be larger than the corresponding bottom meson cross sections:  $4.3 \pm 0.1(\text{stat}) \pm 0.7(\text{syst}) \mu\text{b}$  for  $D^+$ ,  $9.3 \pm 0.1(\text{stat}) \pm 1.1(\text{syst}) \mu\text{b}$  for  $D^0$  and  $5.2 \pm 0.1(\text{stat}) \pm 0.8(\text{syst}) \mu\text{b}$  for  $D^{*+}$  mesons. In the case of the  $D_s^+$  mesons, the integrated production cross section was measured for  $p_T(D_s^+) > 8 \text{ GeV}/c$ ,  $|y(D_s^+)| < 1$  and found to be  $0.75 \pm 0.05(\text{stat}) \pm 0.22(\text{syst}) \mu\text{b}$ . The differential production cross sections ( $d\sigma/dp_T$ ) for all the mesons are depicted in Figure 3. Theoretical predictions (FONLL <sup>12)</sup>) are overlaid in the plots. The error band from the theory curve corresponds to the maximum variation from changing the renormalization scale and the factorization scales between 0.5 and  $2.0 \times \sqrt{p_T^2 + m^2}$ .

## 5 Branching Ratios and $CP$ Asymmetry

The study of the precise structure of the CKM matrix has been guided by measurements of mixing and  $CP$  violation in the neutral  $K$  and  $B$  meson sectors. The Standard Model predictions for the rate of mixing and  $CP$  violation in the charm sector are small, with the predictions in both cases ranging from 0.1% to 1% <sup>13)</sup>. Observation of  $CP$  violation above the 1% level would be strong evidence for physics outside the Standard Model. The SU(3) flavor symmetry

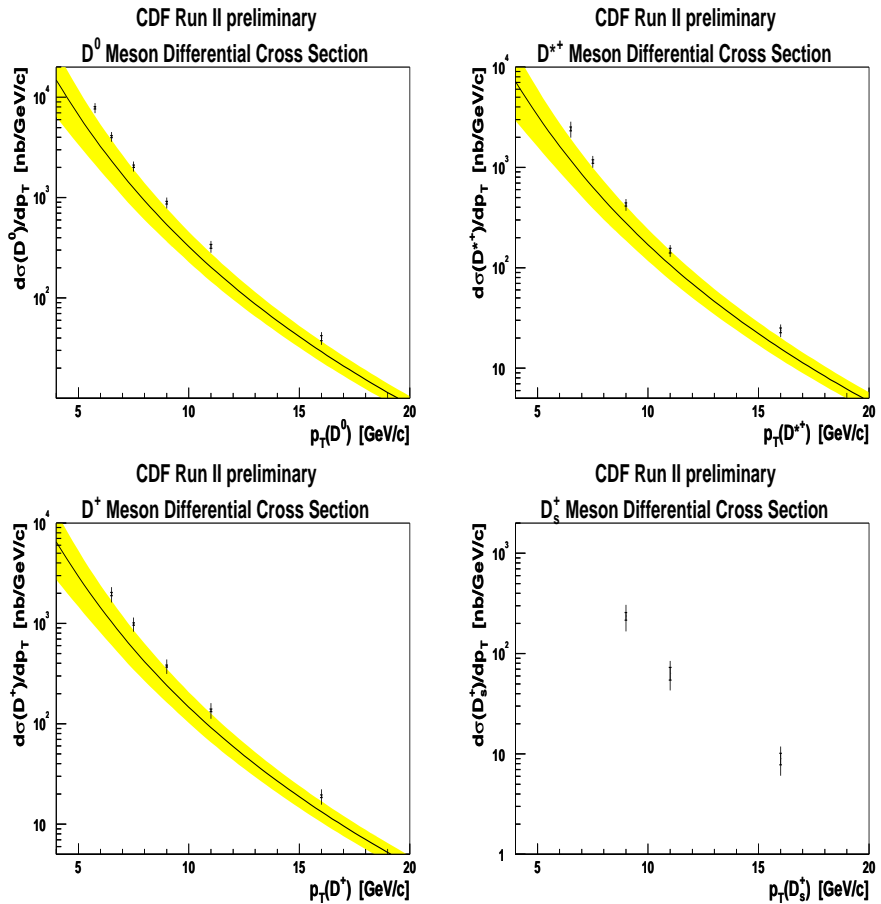


Figure 3: Charm meson differential cross sections for  $D^0$ ,  $D^{*+}$ ,  $D^+$  and  $D_s^+$  mesons, respectively. Theoretical predictions are overlaid upon the measurement results.

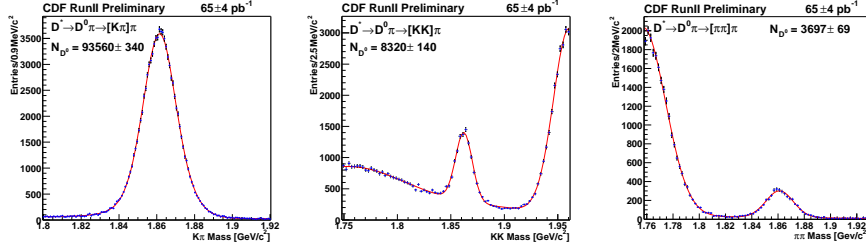


Figure 4: Invariant mass distributions for the three two-body  $D^0$  decays: the dominant  $D^0 \rightarrow K^-\pi^+$ , the Cabibbo suppressed  $D^0 \rightarrow K^+K^-$  and  $D^0 \rightarrow \pi^+\pi^-$ . All three decay modes are reconstructed by requiring that the  $D^0$  comes from the decay  $D^{*+} \rightarrow D^0\pi^+$ .

predicts  $\Gamma(D^0 \rightarrow K^+K^-)/\Gamma(D^0 \rightarrow \pi^+\pi^-) = 1^{+14}_{-8}$ , while the world average value is  $2.88 \pm 0.15^{+8}_{-8}$ . This deviation is most likely caused by large final state interactions (FSI) <sup>15</sup>. In the initial  $65 \pm 4 \text{ pb}^{-1}$  of Run II data, 93 000  $D^0 \rightarrow K^-\pi^+$ , 8 300  $D^0 \rightarrow K^+K^-$  and 3 700  $D^0 \rightarrow \pi^+\pi^-$  decays were reconstructed, as shown in Figure 4. Good signal to background was obtained by requiring that the  $D^0$  always originates from a  $D^{*+}$  decay:  $D^{*+} \rightarrow D^0\pi^+$ . Using these samples of  $D^0$  decays, the following measurements of the ratios of branching ratios were obtained by correcting the raw number of reconstructed candidates by the relative trigger and reconstruction efficiencies::

$$\frac{\Gamma(D^0 \rightarrow K^+K^-)}{\Gamma(D^0 \rightarrow K\pi)} = 9.38 \pm 0.18(\text{stat}) \pm 0.10(\text{syst}) \% \quad (1)$$

$$\frac{\Gamma(D^0 \rightarrow \pi^+\pi^-)}{\Gamma(D^0 \rightarrow K\pi)} = 3.686 \pm 0.076(\text{stat}) \pm 0.036(\text{syst}) \% \quad (2)$$

The direct  $CP$  asymmetries for  $D^0$  decays were found to be  $2.0 \pm 1.7(\text{stat}) \pm 0.6(\text{syst})\%$  for  $D^0 \rightarrow K^+K^-$  decays and  $3.0 \pm 1.9(\text{stat}) \pm 0.6(\text{syst})\%$  for  $D^0 \rightarrow \pi^+\pi^-$  decays.

## 6 Rare Charm Decays

For the flavor changing neutral current decay  $D^0 \rightarrow \mu^+\mu^-$ , the Standard Model predicts a branching ratio of  $Br(D^0 \rightarrow \mu^+\mu^-) \sim 10^{-13}$ . The present experimental limit is  $Br(D^0 \rightarrow \mu^+\mu^-) \sim 4.1 \times 10^{-6}$  from BEATRICE <sup>16</sup> ( $4.2 \times 10^{-6}$  from E771 <sup>17</sup>), 7 orders of magnitude from the prediction.

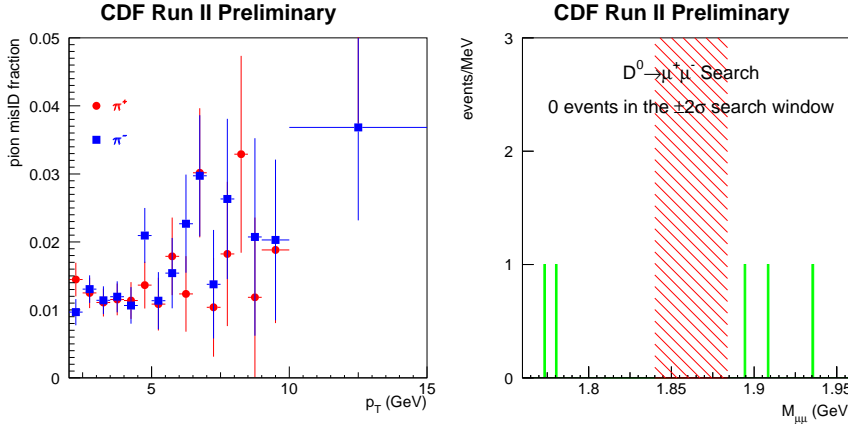


Figure 5: Elements of the  $D^0 \rightarrow \mu^+ \mu^-$  analysis. The left plot depicts the rate at which pions are misidentified as muons, and the right plot shows the absence of events in the search window.

New physics can substantially enhance this mode. In charm meson decays we are constraining couplings to up-type quarks not necessarily constrained by  $B$  decays. This makes  $D^0 \rightarrow \mu^+ \mu^-$  an unexplored region to search for new physics.

Using  $69 \text{ pb}^{-1}$  of Run II data, a search for  $D \rightarrow \mu^+ \mu^-$  decays was performed. As in the  $CP$  asymmetry analysis, the  $D^0$  decays were reconstructed in a clean final state by requiring that they originate from  $D^{*+} \rightarrow D^0 \pi^+$  decays. The kinematically similar  $D^0 \rightarrow \pi^+ \pi^-$  decay was used as a normalization mode. The sources of background for this decay are  $D^0 \rightarrow \pi^+ \pi^-$  events in which both pions are misidentified as muons and combinatorial background. Both the pion misidentification rate and the level of the combinatorial background were measured from a kinematically similar but statistically independent set of events. The estimated number of background events in the search window was  $1.7 \pm 0.7$ . No events were found in the search window, as seen in Figure 5, and a limit was set on the branching ratio:  $Br(D^0 \rightarrow \mu^+ \mu^-) < 2.4 \times 10^{-6}$  at 90% C.L. This is currently the world's best limit on the  $D^0 \rightarrow \mu^+ \mu^-$  branching ratio.

## 7 Summary

The upgraded CDF II detector is back in operation and has gathered around  $65 \text{ pb}^{-1}$  of data which can be used for charm analyses. Due to its ability to trigger

on displaced tracks and vertices, the spectrum of charm results has extended from  $J/\psi \rightarrow \mu^+ \mu^-$  decays to include hadronic decays of  $D^0, D^+, D^{*+}$ , and  $D_s^+$ . With the modest amount of data gathered so far, world class results have already been obtained.

## References

1. R. Blair *et al.* [CDF II Collaboration], FERMILAB-PUB-96-390-E.
2. T. K. Nelson *et al.* [CDF II Collaboration], FERMILAB-CONF-01/357-E.
3. A. Sill *et al.* [CDF II Collaboration], Nucl. Instrum. Meth., A **447**, 1–8, (2000).
4. T. Affolder *et al.* [CDF II Collaboration], Nucl. Instrum. Meth., A **485**, 6–9, (2002).
5. K. T. Pitts *et al.* [CDF II Collaboration], FERMILAB-CONF-96/443-E.
6. W. Ashmanskas *et al.* [CDF II Collaboration], Nucl. Instrum. Meth., A **447**, 218–222, (2000).
7. F. Abe *et al.*, Phys. Rev. Lett. **79**, 572 (1997).
8. K. Hagiwara *et al.*, Phys. Rev. D **66**, 010001 (2002).
9. D. N. Brown *et al.* [CLEO Collaboration], Phys. Rev. D **50**, 1884 (1994).
10. B. Aubert *et al.* [BaBar Collaboration], Phys. Rev. D - Rapid Comm. **65** 091104 (2002).
11. D. Acosta *et al.* [CDF II Collaboration], Phys. Rev. D **65**, 052005 (2002).
12. M. Cacciari, P. Nason, private communication.
13. H. N. Nelson, hep-ex/9908021; A. A. Petrov, hep-ph/0009160; I. I. Bigi, hep-ex/014008; A. F. Falk, Y. Grossman, Z. Ligeti, A. A. Petrov, hep-ph/0110317.
14. M. B. Einhorn and C. Quigg, Phys. Rev. D **12**, 2015 (1975).
15. F. Buccella *et al.*, Phys. Rev. D **51** 3478 (1995).
16. M. Adamovich *et al.* [BEATRICE Collaboration], Phys. Lett. B **408**, 469 (1997).
17. T. Alexopoulos *et al.* [E771 Collaboration], Phys. Rev. Lett. **77**, 2380 (1996).